Fibers and Polymers 2014, Vol.15, No.12, 2480-2488
DOI 10.1007/s12221-014-2480-1

ISSN 1229-9197 (print version)
ISSN 1875-0052 (electronic version)

PAN Fiber Diameter Effect on the Structure of PAN-based Carbon Fibers

Lingqiang Kong[1,2], Hui Liu[2], Weiyu Cao[1], and Lianghua Xu[1]*

[1]*College of Materials Science and Engineering, Beijing University of Chemical Technology, National Carbon Fiber Engineering Technology Research Center, Beijing 100029, China*
[2]*Jilin Petrochemical Company, National Carbon Fiber Engineering Technology Research Center, Jilin 132021, China*
(Received April 21, 2013; Revised September 12, 2013; Accepted September 23, 2013)

Abstract: The oxidation reaction mechanism during the thermal stabilization process of polyacrylonitrile(PAN) fibers was studied to investigate why the skin-core structure formed easily after the thermal stabilization of PAN fibers was elaborated. And it was found that the heterogeneity of the fibers was poor. In order to achieve a uniform structure after the stabilization treatment, the fiber diameter was systematically reduced. Three PAN fiber samples with different diameters were selected, and they were treated by thermal stabilization and carbonized under the same conditions. The stabilized samples and carbon fiber samples with different diameters were analyzed by differential scanning calorimetry (DSC), fourier transform infrared spectroscopy (FTIR), X-ray diffraction (XRD), Raman spectroscopy, and elemental analysis. The results show that: the skin-core structure of the PAN fiber with the smallest diameter was completely eliminated by stabilization, and the heterogeneity was better. Meanwhile, C|N bonding also decreased, and the cross-linking reaction was easier to happen to form a large network molecular structure in the fiber with smaller diameter. The degree of graphitization of carbon fibers was higher when the diameter of fibers was reduced, and the relative carbon content increased. Crystallite size parameters were also affected when the diameter of fibers was reduced, with larger d_{002}, lower Lc and increased La. In addition, the graphitization degree, as well as the carbon content was higher in the carbon fiber with smaller diameter.

Keywords: PAN-based carbon fiber, PAN fiber diameter, Skin-core structure, Crystallite size

Introduction

Recent studies have established that PAN fibers, used on a large scale in textile industry, are one kind of the most suitable fibers for the production of high performance carbon fibers. Through the stabilization and carbonization, PAN fibers are made into PAN-based carbon fiber [1-4]. In the stabilization process skin-core structures reduce the homogeneity of fibers. With the development of the carbon fiber technology, a variety of high-performance PAN-based carbon fibers have emerged. Reducing the diameter of PAN fibers is also an attractive topic for the carbon fiber researchers, and most of high-performance carbon fibers in the world have small diameters. Thus, investigating the effect of size on structure formation in PAN-based carbon fibers is particularly important.

The performance of materials depends on their structure. Carbon fibers with different diameters exhibit different mechanical properties, so there must be some differences in the structures of carbon fibers with different diameters. Through analysis of the stabilized samples and carbon fiber samples with different diameters, the structural characteristics of carbon fibers with different diameters have been investigated.

Experimental

Materials

Three PAN fiber samples with different diameters, produced under identical conditions, were used. The fibers were generated by free radical polymerization, by using the copolymerization of acrylonitrile (AN, 99 %wt) and itaconic acid (IA, 1 %wt). After stabilization and carbonization, the test samples were obtained.

Stabilization conditions: 210-270 °C/gradient heating/ 90 min/air atmosphere.

Carbonization conditions: (1) low temperature carbonization: 400-700 °C/gradient heating/120 s/nitrogen atmosphere, (2) high temperature carbonization: 1500 °C/90 s/nitrogen atmosphere.

The diameters of fibers and sample numbers are shown in Table 1.

Apparatus and Procedures

Differential scanning calorimeter (DSC), FT-IR spectrophotometer, elemental analysis, X-ray diffraction, raman spectroscopy, microscopy and nuclear magnetic resonance were used to analyze the samples.

Differential scanning calorimeter (TA Company, Model Q100) was used to analyze sample A1, A2 and A3 under a nitrogen atmosphere. The gas flow rate was 50 ml/min; temperature range was 40-400 °C, under the heating 10 °C/min.

Table 1. The diameter of the fibers and the sample number

Diameter of original PAN fibers (μm)	Stabilization fibers	Carbonization fibers	Diameter of carbon fibers (μm)
8.6	A1	B1	5.4
6.9	A2	B2	4.5
6.1	A3	B3	4.0

*Corresponding author: xulh@mail.buct.edu.cn

A FT-IR spectrometer (Nicolet, Model 5700) was used, averaging 100 scans. The transmission spectra was measured by KBr pellet prepared with finely powdered fiber samples. The scan range was 400-4000 cm^{-1}, with a resolution of 0.09 cm^{-1}. The scan results were used to calculate the relative cyclization rate (ROF) of each sample [5], using formula 1 as follows:

$$ROF = \frac{I_{C=N} \cdot f}{I_{C=N} \cdot f + I_{C \equiv N}} \quad (1)$$

where $I_{C=N}$ represents the intensity of stretching vibration of conjugated -C=N- groups at 1580 cm^{-1}; $I_{C|N}$ represents the intensity of stretching vibration of -C|N groups at 2240 cm^{-1}, and $f=E_{C|N}/E_{C=N}$, where E represents the respective absorptivity constant. Under normal circumstances, we use f=0.29 [5].

The C, H, N composition of the carbonized samples was performed on an elemental analyzer (Elementar, model Vario EL II).

Changes in crystal structure that occurred during heat treatment were determined using an X-ray diffraction analyzer (model D/max-2550PC) operating at 40 kV and 40 mA with Ni-filtered Cu K_α radiation. The multifilament yarns were bundled and fixed on an X-ray fiber holder that was 10 mm wide (equatorial scan) and 20mm long in the vertical (meridian scan) directions. Data was collected over the 2θ range from 10 to 90° at 1°min^{-1}. The diffraction peak positions and the full widths at half maximum (FWHM) were used to calculate the crystallite size by the Scherrer equation, as formula 2 shows:

$$L(hkl) = \frac{K\lambda}{B \cdot \cos\theta} \quad (2)$$

where θ is the diffraction peak position of the (hkl) plane, we can get θ from the diffraction curve clearly, λ= 0.15406 nm is the wavelength of the X-rays. B is the FWHM (in radians) of the peak, it is the widths of the peak at half of peak height, and K is the Scherrer geometric or shape factor. The crystallite thickness (Lc) perpendicular to the fiber axis was calculated using the (002) diffraction peak of the equatorial scan, and the crystallite correlation length (La) along the fiber axis was determined from the (100) diffraction peak of the meridian scan. The shape factor K was 0.9 for Lc and 1.84 for La [6].

Raman spectroscopy was carried out using a Renishaw RM2000 Raman spectrometer (Renishaw Plc, UK) attached to an Olympus optical microscope, using a He-Ne laser (wavelength=514.5 nm). The samples were deposited on glass slides. The 20× objective lens of the microscope was used both to focus the laser beam on the specimen and to collect the scattered radiation. The laser beam was polarized parallel to the fiber axis and focused to give a 5 mm diameter spot on the fiber surface, and a high sensitivity Renishaw charge-coupled device camera was used to collect the spectral data.

Optical microscopy was used for observing the skin-core structure image of the samples. Optical microscope (Olympus, CX21BIM-SET5) was operated at an eyepiece of 10× and objective of 20× magnifications.

High resolution solid state ^{13}C NMR spectra was collected for the A1, A2 and A3 samples on Bruker (AV-300), at 73.5 MHz, under a loop delay time of 5 s and a contact time of 3 ms. 300-3175 scans were performed, using a 4 mm CP/MAS probe at a rotor rotation rate of 8.5 kHz.

Density was measured at 25 °C in a density gradient column (Lloyd, UK), prepared with a mixture of n-heptane and carbon tetrachloride, which gave a density gradient from about 1.29 at the top to 1.45 g·cm^{-3} at the bottom.

Results and Discussion

Characteristics of the Radial Structure Evolution of PAN Fibers during the Stabilization Process

Thermal stabilization of PAN fibers is usually carried out in air, generally using a gradient heating to control the temperature over the range of 200-300 °C and using appropriate tension to maintain orientation. Cyclization, oxidation, dehydrogenation and cross-linking reactions occur inside the fibers [7], resulting in a structure which is not easy to crack in the carbonization process.

Based on previous studies, Fitzer [8] and Bashir [9] summarized the reaction mechanism of cyclization and dehydrogenation during the thermal stabilization process in the air, as Figure 1 shows, the PAN macromolecules formed into cyclic structure by the dehydrogenation reaction and the intramolecular cyclic polymerization.

Figure 2 shows the DSC exothermic curves of PAN fibers in the oxygen medium (air) and the inert medium (nitrogen). From this figure, obviously, there are some differences of the DSC curves between the two different atmospheres. The curve under the inert medium has only one exothermic peak, and the peak shape is narrow and sharp.

Compared with the DSC curve which is taken under the inert medium, the DSC curve in the air condition shows a double peak. The differences of these two curves under different atmospheres show that the thermal stabilization process can react differently between in the air and nitrogen.

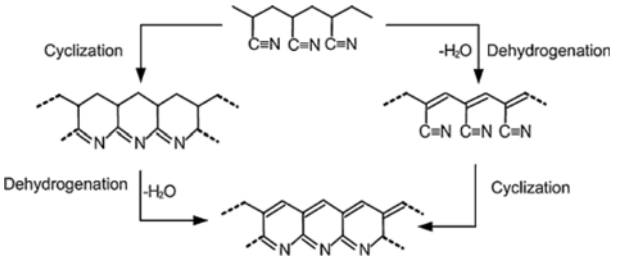

Figure 1. Reaction mechanism of PAN fibers in process of thermal stabilization.

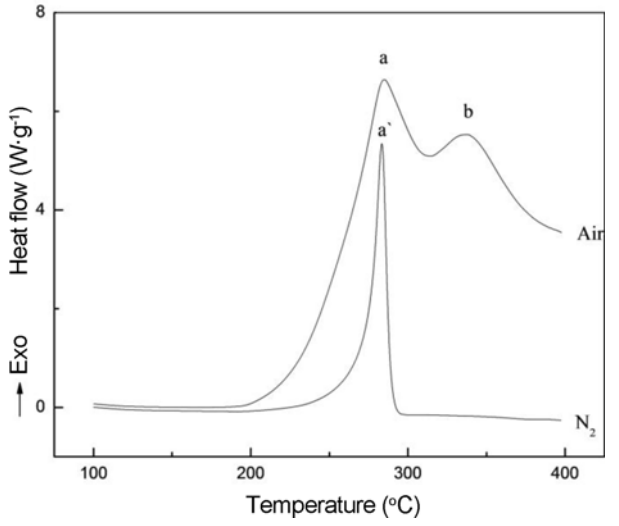

Figure 2. DSC curves of PAN precursor in air and nitrogen atmosphere (heating rate: 10 °C/min, gas flow: 50 ml/min).

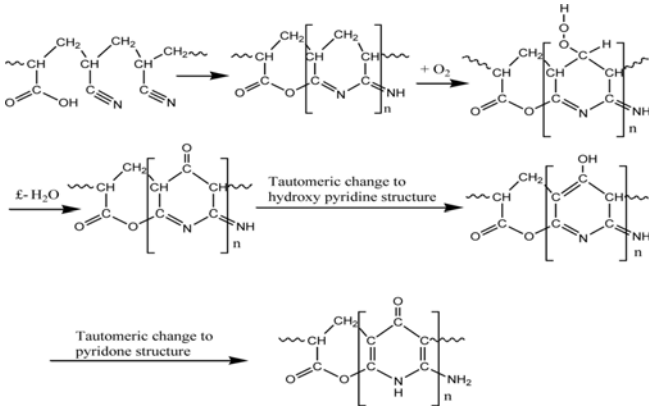

Figure 3. Oxidation mechanisms of PAN fibers in process of thermal stabilization.

Gupta *et al.* [10] studied the chemical reactions which peak a and peak b represented, in their opinion, peak a represented the cyclization reaction while peak b represented the oxidation reaction, and the cyclization reaction is the precondition of the oxidation reaction.

Combining the messages from Figure 1 and Figure 2, it can be concluded that the thermal stabilization process gradually forms a multilevel structure. In thermal environment, the cyclization reaction of PAN molecules first occurs, causing the original structure changed into the first level structure by the catalysis of oxygen contained in the environment. After forming into the cyclic structure, PAN molecules react easily with the oxygen in the air and form new structures. This viewpoint was proved by Watt and Johnson [11], as shown in Figure 3.

On one hand, the reaction with oxygen intervenes the developing of the fibers' radial structure, on the other hand, the reactive part keeps reacting into higher level structure by

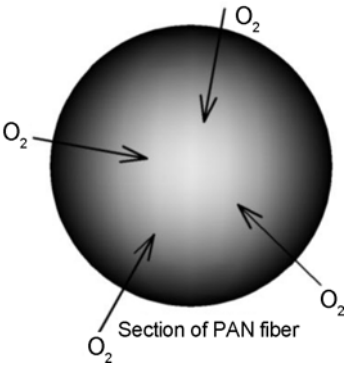

Figure 4. The diagrammatic sketch of oxygen permeate in fiber cross-section.

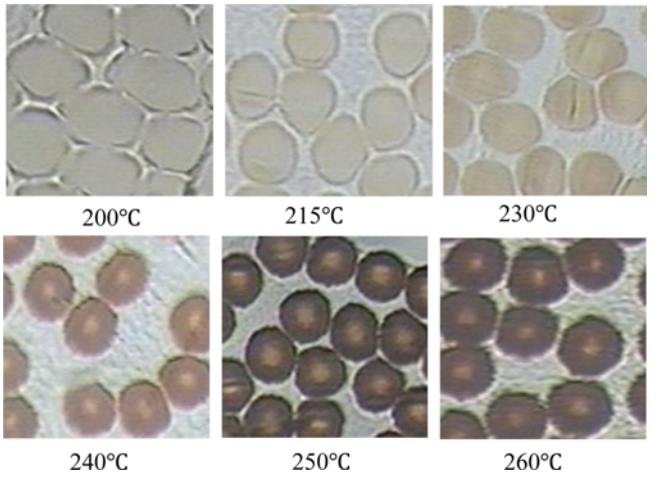

Figure 5. The skin-core photos of PAN fibers prepared at different thermal stabilization temperatures.

the catalysis or direct participation of oxygen. This procedure depends on the oxygen penetration effect within the fibers. The oxygen penetration effect is developing from the surface to the inside of the fibers, as shown in Figure 4. Firstly, the ladder-shaped dense layer formed on the surface of the fibers, and this layer prevents the oxygen from spreading to the inside of fibers. As the reaction continues, the inhibition effect of oxygen becomes stronger while the density layer grows thicker. Then the surface of the fibers continuous to react with oxygen and more complicated oxydic structure forms. Meanwhile, the inside of the fibers is in anaerobic condition, so the reaction is inhibited. The total processes lead to the formation of the skin-core structure.

Figure 5 is the skin-core structure image of the sample at different temperatures by the gradient-heating thermal stabilization. It can be seen that the color of the fibers is changing from light to dark as the reaction progresses. After thermal stabilization, the skin-core structure in the fiber is formed obviously.

The appearance of the skin-core structure largely affects

the uniformity of the precursors and the performance of the final carbon fibers. Thus, eliminating the skin-core structure becomes an important issue. During the thermal stabilization process, temperature and thermal treatment time are two important technological parameters, which can both affect the fibers' radial structure to some extent. After a lot of experiments, it can be found that changing the temperature and thermal treatment time during thermal stabilization process can reduce the core proportion of the skin-core structure, but can not eliminate the skin-core structure. In addition, considering the output and cost of the industrial production, the technological parameters must be set within a reasonable scope. Thus, eliminating the skin-core structure should be considered from the angle of the fibers diameter reduction. Oxygen can spread easily from the surface to the core in small diameter fibers, and benefits the homogeneity improvement of the fibers.

PAN Fiber Diameter Effect on the Structure Formation of PAN Fiber during the Stabilization Process

PAN Fiber Diameter Effect on the Radial Structure of PAN Fiber during Stabilization Process

Figure 6 shows the skin-core photos of the stabilized PAN fibers with different diameters. The skin-core structure is eliminated by reducing the diameter of the fiber, and the heterogeneity of the internal structure of the fibers is improved. This is because oxygen can more effectively penetrate into the smaller diameter fibers.

PAN Fiber Diameter Effect on the Aggregation Structure of the PAN Fiber during Stabilization Process

Figure 7 shows the DSC thermograms of the original PAN fibers and the stabilized PAN fibers with different diameters.

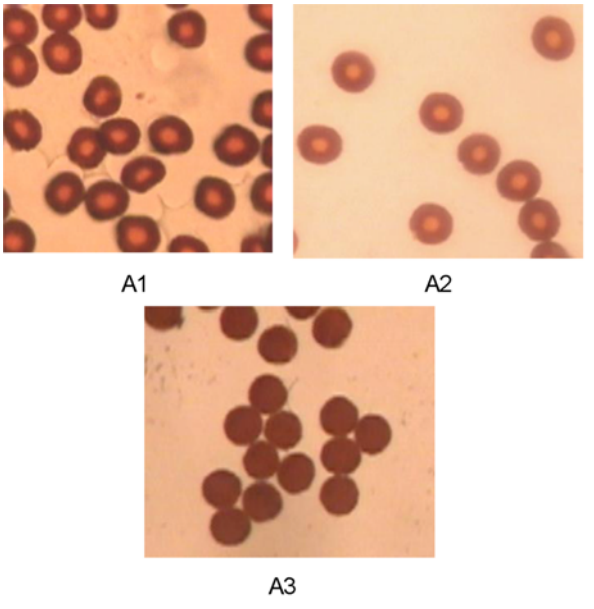

Figure 6. The skin-core photos of PAN fiber with different diameter after stabilization.

And Figure 7(a) show the original PAN fibers and the stabilized PAN fibers together in one graph, because of the original PAN fibers' same component, there was difference among the three original PAN fibers. Figure 7(b) shows the stabilized PAN fibers with different diameters. The exothermic peak decreases as the diameter of fiber decreases, and the

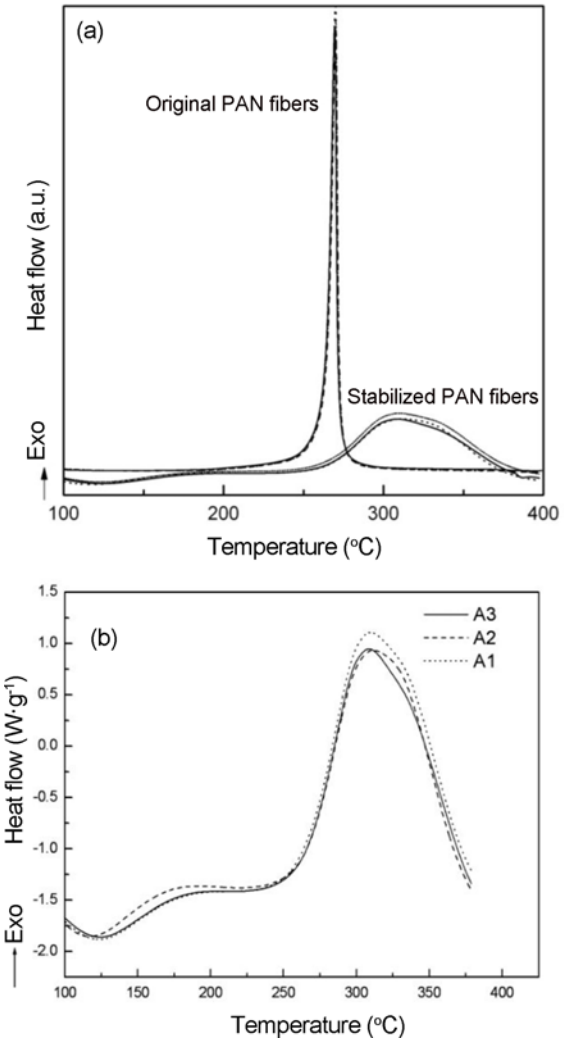

Figure 7. (a) DSC spectra of the original PAN fibers and the stabilized PAN fibers with different diameters in nitrogen atmosphere and (b) DSC spectra of the stabilized PAN fibers with different diameters in nitrogen atmosphere.

Table 2. The exothermic heat values of the stabilized PAN fibers with different diameters under a nitrogen atmosphere

Sample	Exothermic heat ($J \cdot g^{-1}$)
Original PAN fiber	549
A1	340.2
A2	325.6
A3	320.5

Table 3. The density values of the stabilized PAN fibers with different diameters

Sample	Density ($g \cdot cm^{-3}$)
A1	1.3591
A2	1.3596
A3	1.3614

exothermic heat values of three samples are shown in Table 2. This means the cyclization degree in smaller diameter fibers is relatively higher. This is because oxygen helps catalyze cyclization during stabilization. Thus, cyclization is increased in smaller fibers due to the increased oxygen penetration.

The densities of the three stabilized samples are shown in Table 3. The density increases as the diameter of fibers decreases. The core material of the skin-core structure has a lower density, and as more material is transformed into smaller diameter fibers, the density increases.

PAN Fiber Diameter Effect on the Chemical Structure of PAN Fiber during Stabilization Process

Fitzer *et al.* [8] proposed a reaction mechanism for the thermal stabilization of PAN fibers and described the nature of the perfect stabilized structure. It consists of 40 % of acridine rings, 30 % of pyridine rings and 20 % of hydrogenated naphthyridine rings with the remaining 10 % consisting of a variety of minor structures, shown in Figure 8.

This mechanism takes into account the cyclization, dehydrogenation and oxidation reactions which occur in the thermal stabilization process, and is recognized by many researchers. It includes a conversion of -C≡N bonds to cyclized -C=N- bonds during the thermal stabilization process. The IR spectra of three stabilized PAN fibers with different diameters were shown in Figure 9. The peak represents -C=N- groups at 1580 cm^{-1} and the peak represents -C≡N groups at 2240 cm^{-1} were marked in Figure 9. The intensity of stretching vibration of conjugated -C=N- groups and conjugated -C≡N groups of the stabilized PAN fibers with different diameters were used to calculate the relative cyclization rate (ROF), and to compare the diameter of fiber by the ROF. The results were shown in Figure 10.

Figure 10 shows that the relative cyclization rates of samples decrease as the fiber diameter increases. The relative cyclization rate can be used to determine the extent of the cyclization reaction by the relative proportions of -C≡N and C=N. Therefore, from the figure, it can be seen that increasing the fiber diameter effectively improves the rate of -C≡N bond

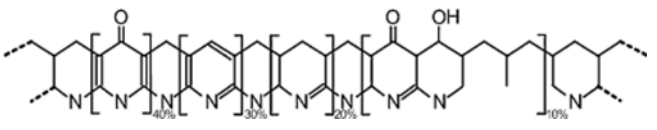

Figure 8. The diagrammatic sketch of the thermal stabilization structure of PAN fibers.

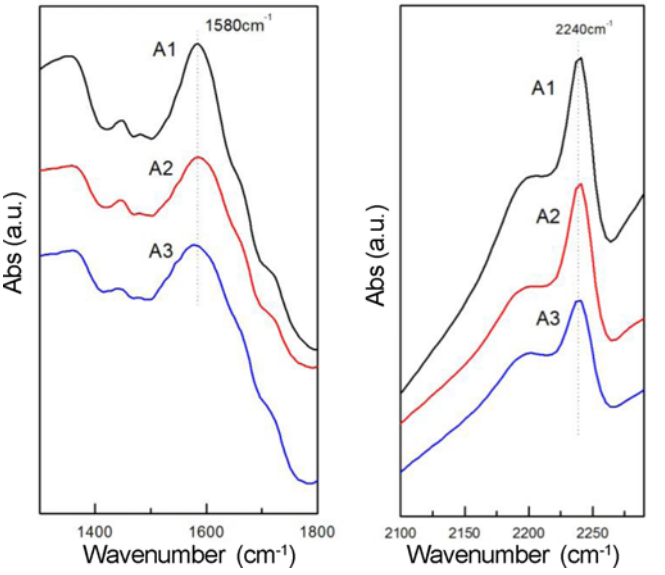

Figure 9. FT-IR spectra of the stabilized PAN fibers with different diameters.

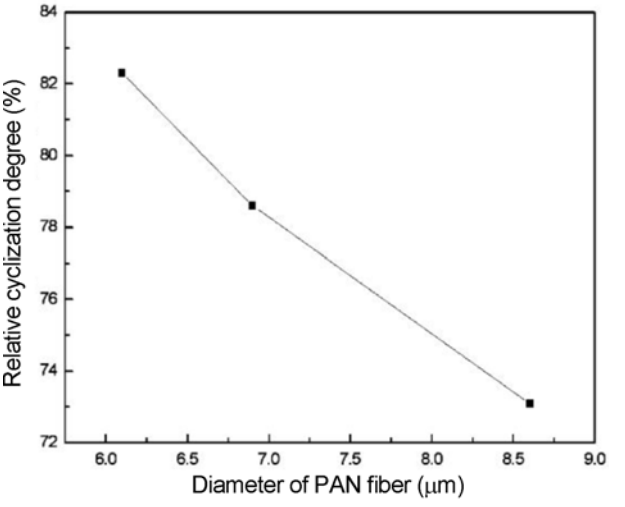

Figure 10. The relationship between the diameter and the relative cyclization rate.

conversion into -C=N- units, and allows the cyclization process to complete.

Figure 11 shows the solid state ^{13}C NMR CP/MAS spectra of the stabilized samples with different diameters. The peak at 30 ppm (a) represents CH and CH2 carbon atoms. The peak at 116 ppm (b) represents C=C carbon atoms and it is identifiable that carbon atoms are not substituted with hydrogen atoms. The peak at 122 ppm (c) represents the -C≡N carbon atoms and the peak at 139 ppm (d) represents C=C carbon atoms where at least one substituent is the hydrogen atom. The peak at 153 ppm (e) represents C=N

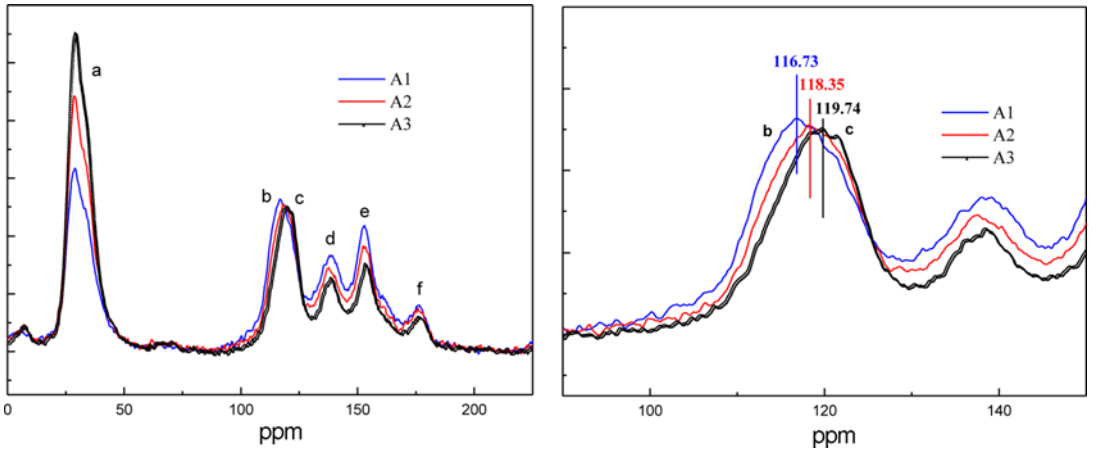

Figure 11. NMR spectra of the stabilized PAN fibers with different diameters.

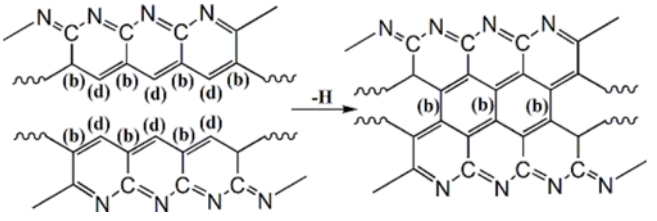

Figure 12. The diagrammatic sketch of the intramolecular cyclization reaction by dehydrogenation.

carbon atoms which formed from -C⎪N units (c). Finally the peaks at 177 ppm (f) and above represents the carbon atoms of C=O units [12]. On the peak at 116 ppm, there is a shoulder peak at 118 ppm. As the fiber diameter decreases, the peak intensity at 116 ppm becomes stronger relative to the peaks at 118 and 122 ppm. This means the -C⎪N bond content decreases as the diameter of fiber decreases, and the C=C bonds are more common in the structure. Thus decreasing the diameter improves conversion of -C⎪N bonds to-C=N- bonds.

The intramolecular cyclization reaction dominates during thermal stabilization of PAN fibers. But in the case of sufficient and concentrated heat, the cross-linking will happen between molecules by dehydrogenation, and then the macrocyclic molecules with a higher degree of cross-linking are formed, as shown in Figure 12. During this process, C=C(d) carbon transforms into C=C(b) carbon in molecules by dehydrogenation, hence, the relative content of C=C(b) carbon in the C=C structure increases, and this trend also shows that the dehydrogenation cross-linking reaction with higher degree exists in the intermolecular PAN fibers.

The peak separation method was applied on the peaks representing C=C(b), -C⎪N(c), and C=C(d) in NMR spectrum, as shown in Figure 13. The peak area (S_b) of C=C(b) and the peak area (S_d) of C=C(d) were calculated, the ratio of S_b and S_d was used to show the relative proportion of the two

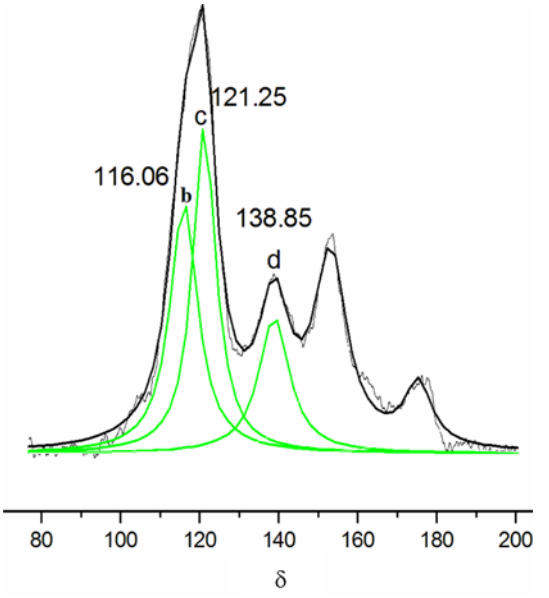

Figure 13. The diagrammatic sketch of the application of the Peak separation method on NMR spectrum.

Table 4. The numerical value of the S_b/S_d of thermal stabilization fibers with three diameters

Sample	S_b/S_d
A1	1.01
A2	1.17
A3	1.52

aromatic carbon atoms, and the numerical value may represent the degree of intermolecular cross-linking in the sample.

The peak separation method of NMR was applied to thermal stabilization fibers with three diameters, the data were collected in Table 4. It can be seen that the numerical

value of the S_b/S_d increased as the diameter of the PAN fibers decreased. Therefore, it can be concluded that more intermolecular cross-linking reaction occurred in small diameter fibers under the same heat stabilization process.

There are two main reasons for this phenomenon. First, PAN fibers with smaller diameter have an advantage in heat and mass transfer during heat treatment, and the thorough penetration of oxygen makes the skin and the core un-differentiated. In addition, oxygen plays a catalyst role in promoting the cyclizing reaction, resulting in the reaction of forming the primary structure of fibers with smaller diameter is fully completed, and that lays the foundation for the subsequent reaction. The second reason is the reaction activation energy. The reactions are carried out from the surface to the centre of the fiber, and that will consume the absorbed energy, impacting the transition from the primary structure to the secondary structure. Therefore, under the same thermal stabilization condition, the reaction of forming the primary structure in fibers with smaller diameter is fully completed. The concentrations of energy promote the transition from the primary structure to the secondary structure, so that the overall pre-oxidation process is faster.

By analyzing the skin-core structure, the aggregation structure and the chemical structure of thermally stabilized fiber samples with three diameters, the sample with smaller diameter possess better homogeneity, and more completed reaction as the thermal stabilization is carried out, and the cross-linking reaction is easier to happen, forming a large molecular network structure in the fiber with smaller diameter.

PAN Fiber Diameter Effect on the Structure of PAN-Based Carbon Fiber

The Correlation between the Diameter of Fiber and the Degree of Graphitization in PAN-based Carbon Fibers

Figure 14 shows the Raman spectra of carbon fibers with

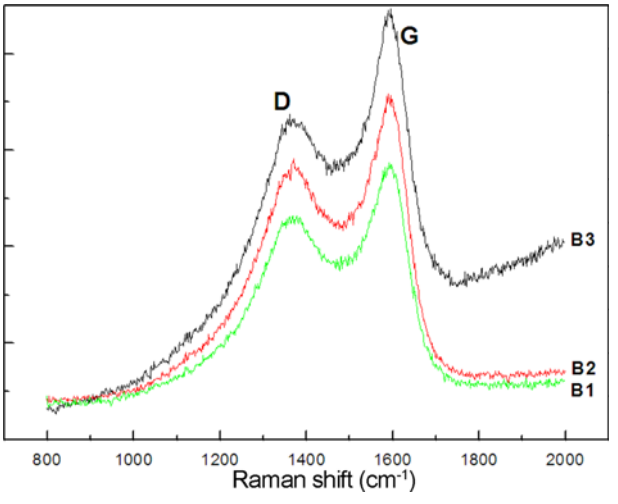

Figure 14. Raman spectra of carbon fibers with different diameters.

Table 5. Raman data of the carbon fibers with different diameters

Sample	D (cm^{-1})	G (cm^{-1})	R
B1	1372.3	1587.1	0.846
B2	1373.6	1587.8	0.839
B3	1373.6	1588	0.793

different diameters. There are two characteristic peaks which indicate different chemical structures; the D peak near 1320 cm^{-1} indicates a disordered structure, and the G peak near 1575 cm^{-1} indicates a graphite structure, and the peak position of single-crystal graphite in Raman spectra at 1580 cm^{-1}.

We can use the formula $R=I_D/I_G$ (I_D and I_G represent integral intensities of the D and G peaks, respectively) to calculate the relative content of sp^2 hybrid carbon atoms in the carbon fiber, which is the degree of graphitization [13,14]. Smaller R values mean a higher degree of graphitization of the carbon fiber. The G peak intensity of the B3 sample is larger, and as the diameter increases, the G peak intensity becomes smaller. The Raman shifts of the G and D peaks, and the R values of the samples, are listed in Table 5.

From Table 5, it can be seen that the G peak of each carbon fiber is blue shifted in comparison with single-crystal graphite. The R value of the carbon fiber increases as the diameter of fiber increases, meaning the larger the diameter is, the lower the graphitization of the carbon fiber will be. This is because the small diameter carbon fibers have superior heat and mass transfer in the thermal treatment process, and thus the degree of heat treatment is relatively high. Oxygen penetrating into the core of the smaller fibers becomes easier in the process of stabilization, and small molecule byproducts can leak out of the fiber more easily. This means the stabilization process progresses further. At the same time, the better heat transfer leads to more cross-linking of the fiber, so that the larger molecules are formed [12]. After carbonization, these large molecular structures become larger graphite sheets. Although the edges of these graphite sheets are not graphitic, most of the sheet is sp^2 carbon. As the sheets get bigger, the proportion of sp^2 graphic carbon gets bigger. Thereby, the degree of graphitization in the carbon fiber increases.

The Correlation between the Diameter of Fiber and Elemental Content of PAN-based Carbon Fiber

Table 6 shows the elemental content of the PAN-based carbon fibers with different diameters. The relative carbon content increases and the nitrogen and hydrogen content

Table 6. Elemental analysis of the carbon fibers with different diameters

Sample	C (%)	N (%)	H (%)
B1	95.970	3.841	0.195
B2	96.430	3.412	0.190
B3	96.610	3.172	0.136

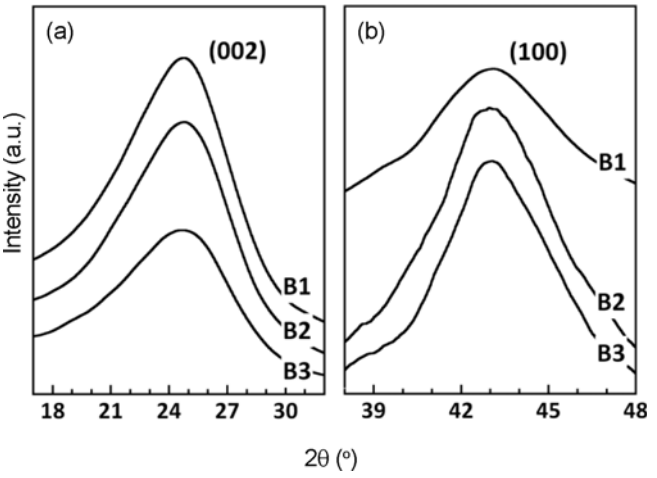

Figure 15. X-ray diffraction spectra of three carbon fibers with different diameters.

decreases as fiber diameter decreases. It is believed that the degree of stabilization in the small diameter fibers is higher. This lays a better foundation for the removal of non-carbon elements. In addition, there are small amount of non-carbon elements that need to be removed. The diameter of the fiber affects the outward diffusion of small molecules from the center of the fiber. A smaller fiber makes this process easier as the relative carbon content increases.

The Correlation between the Diameter of Fiber and Crystallite Size of PAN-based Carbon Fiber

Figure 15 shows the X-ray diffraction spectra of three carbon fibers with different diameters. Peaks represents (002) and (100) are placed together, and the peak parameters can be got by analyzing the figure; Table 7 shows the crystallite size of PAN-based carbon fibers with different diameters, and the correlation between the diameter of fiber and crystallite size of PAN-based carbon fiber are shown in Figure 16. As the diameter of fiber decreases, d_{002} becomes larger, Lc becomes smaller and La increases. This means the order within the graphite structure of carbon fiber decreases, the stack thickness of the graphite layers decreases, but the size of graphite layers increases. This is because reducing the diameter of the fiber improves mass and heat transfer, and the increasing of the polycondensation and cross-linking processes in the fiber improve the growth of the graphite layers.

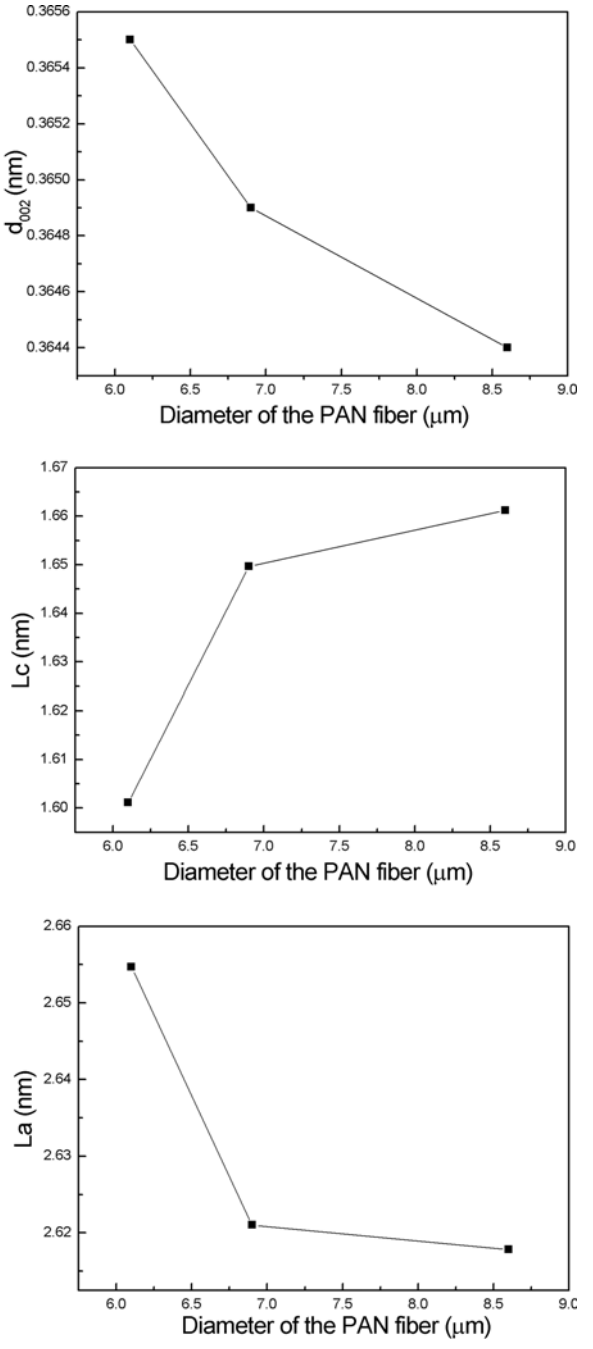

Figure 16. The correlation between the diameter of fiber and crystallite size of PAN-based carbon fiber.

Table 7. Structural sizes in the carbon fibers with different diameters

Sample	$2\theta_1$	d_{002} (nm)	B_1	Lc (nm)	$2\theta_2$	B_2	La (nm)
B1	24.422	0.3644	5.4391	1.6612	43.181	6.4206	2.6178
B2	24.384	0.3649	5.4768	1.6497	43.085	6.4113	2.6210
B3	24.345	0.3655	5.6426	1.6011	43.163	6.3317	2.6547

Conclusion

There were some correlations between the structure of PAN-based carbon fibers and the diameter of the fiber when the three samples were exposed to the same stabilization and thermal processes. PAN fibers with small diameters showed improved mass and heat transfer, which allowed the stabilization and carbonization processes to fulfill completely, and allowed small molecule byproducts to escape more easily. Small diameter fibers completely eliminated the skin-core structure of PAN fiber after stabilization and improved the inhomogeneity. Characteristic reactions of the stabilization process such as cyclization reactions increased as residual -C⎪N bonds decreased, and the cross-linking reaction was easier to happen to form a large molecular network structure in the fiber with smaller diameter. The degree of graphitization was higher within smaller diameter fibers and the relative content of carbon element increased. Crystallite size parameters were also affected by the diameter of the fibers when the order of the graphite structure and the stack thickness decreased, but the size of the graphite layers was improved.

References

1. O. P. Bahl, R. B. Mathur, and K. D. Kundra, *Fiber Sci. Tech.*, **15**, 147 (1981).
2. M. C. Yang and D. C. Yu, *J. Appl. Polym. Sci.*, **59**, 1725 (1996).
3. J. B. Donnet and R. C. Bansal, "Carbon Fibers", 2nd ed., pp.10-13, Marcel Dekker, NY, 1990.
4. J. Mittal, R. B. Mathur, and O. P. Bahl, *Carbon*, **35**, 1713 (1997).
5. G. L. Collins, N. W. Thomas, and G. E. Williams, *Carbon*, **26**, 671 (1988).
6. J. W. Jeffrey, "Methods in X-ray Crystallography", Academic Press, NY, 1971.
7. M. S. A. Rahaman, A. F. Ismail, and A. Mustafa, *Polym. Degrad. Stab.*, **92**, 1421 (2007).
8. E. Fitzer, W. Frohs, and M. Heine, *Carbon*, **24**, 387 (1986).
9. Z. A. Bashir, *Carbon*, **29**, 1081 (1991).
10. A. K. Gupta, D. K. Paliwal, and P. Bajaj, *J. Appl. Polym. Sci.*, **58**, 1161 (1995).
11. W. Watt and W. Johnson, *Nature*, **257**, 210 (1975).
12. T. Usami, T. Itoh, H. Ohtani, and S. Tsuge, *Macromolecules*, **23**, 2460 (1990).
13. L. Nikiel and P. W. Jagodzinski, *Carbon*, **31**, 1313 (1993).
14. M. Yoshikawa, N. Nagai, and M. Matsuki, *Phys. Rev. B*, **46**, 7169 (1992).